Physics of the Diffuse Universe

Professor Crystal L. Martin
UC Santa Barbara

Outline for HII Regions

- Thermal Equilibrium
- Stromgren Sphere
- Recombination Line Spectrum

Resources

- Draine ch 27, 15, 14
- Osterbrock
  - Astrophysics of Gaseous Nebulae and AGN
  - Ch 2, 3, 4
- Dopita & Sutherland
  - Ch 9, 10

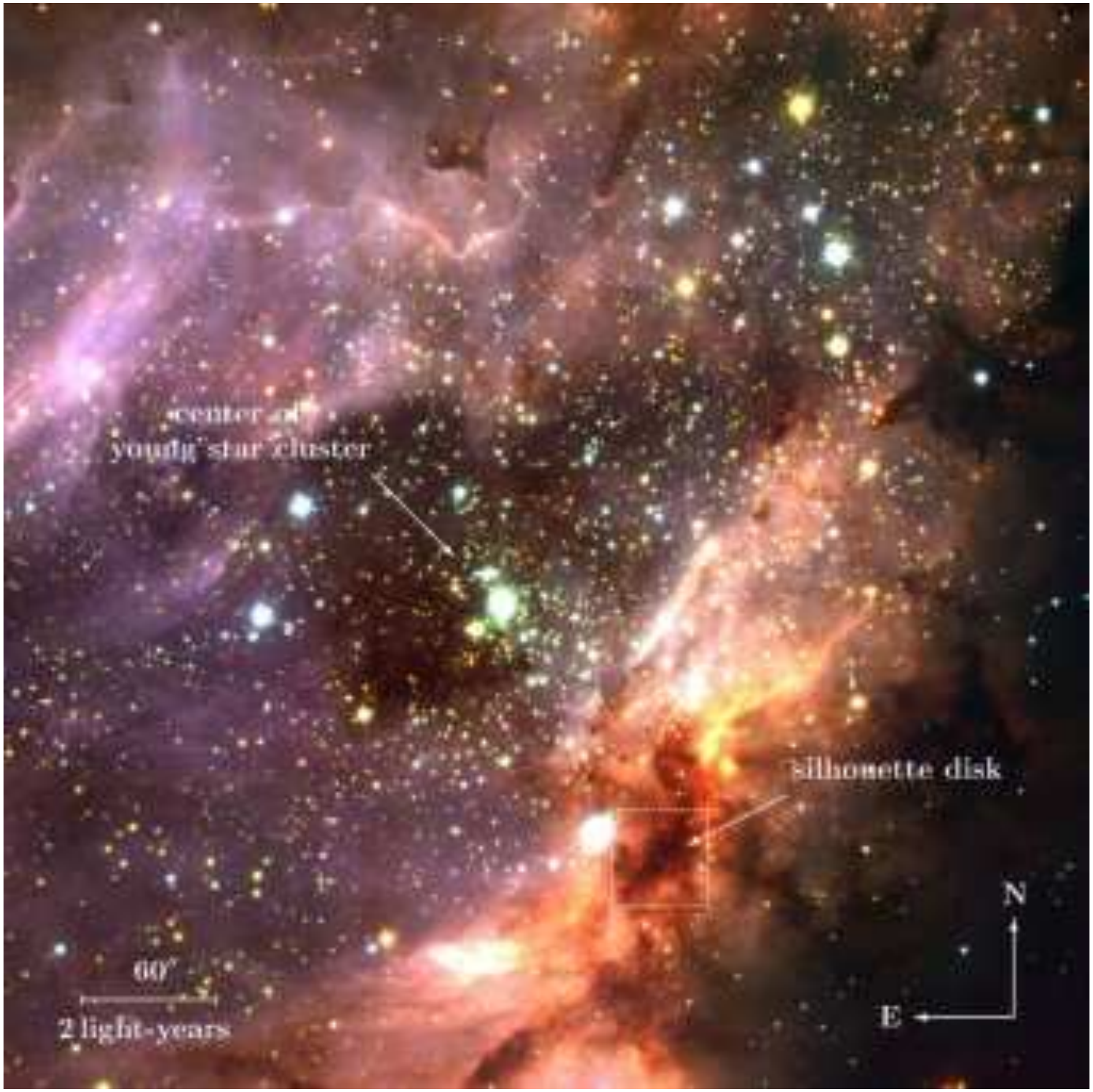
center of
young star cluster
silhouette disk
N
E
60"
2 light-years

30 Doradus

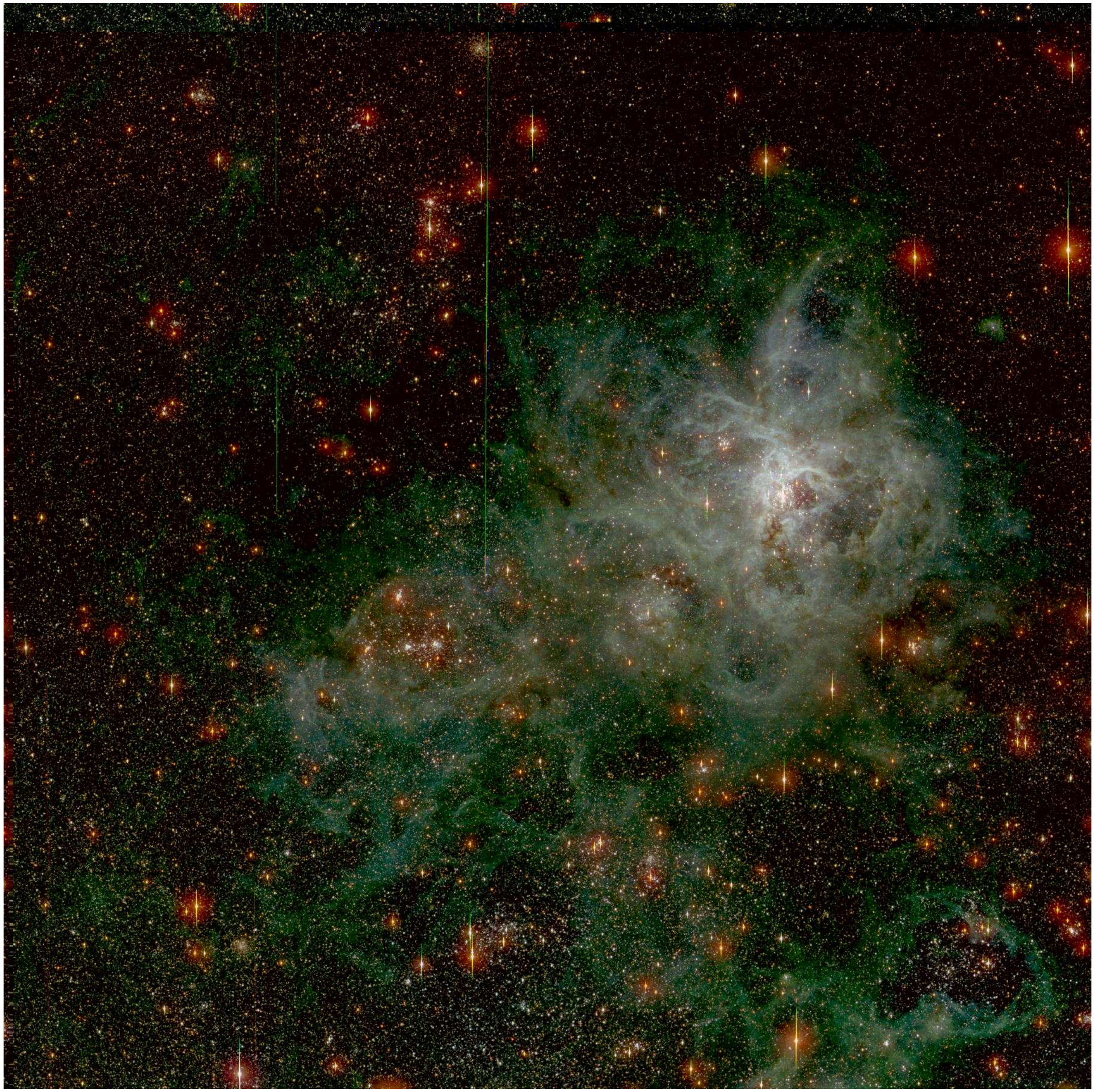

Nestled in the center of M42 is a group of stars, known as the Trapezium, which have formed from the gas in the nebula.The stars of the Trapezium are young blue stars. It is their energy which makes the nebula glow.

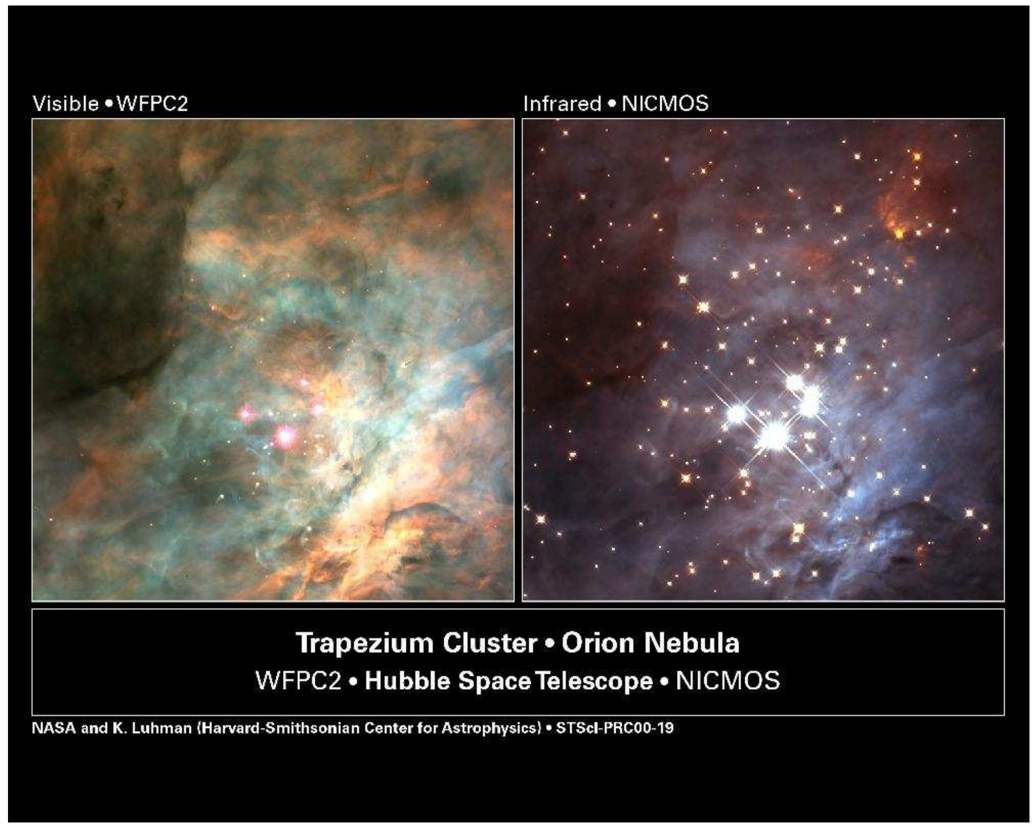

Thermal Equilibrium

- Mean energy of a photoelectron is kT^*
- Depends only on the shape of the Spectral Energy Distribution (SED)
- The rate of photoelectron production depends on the strength of the radiation field.
- Mean energy of a recombining e- is kT_e
- $\alpha_{Rec} \sim \sigma_{Rec}\, v \sim v^{-1} \sim T^{-1/2}$
- $\sigma_{Phot} \sim \nu^{-3}$
- SED hardens with increasing distance from a star

Thermal Equilibrium of HII Regions

- Plot heating rate and cooling rate vs. temperature
- The intersection of these functions gives the equilbrium temperature
- The rapid increase in cooling rate with T, and the decrease in heating rate with T, acts as a 'thermostat' to regulate the HII region T to a narrow range (roughly 8000 K to 20,000 K) over a very wide range of heating rates (MS stars, PNe, AGN, etc.)

Photoionization Equilibrium

- Lyman continuum photon luminosity
- Pure H Nebula
- Nebulae with H and He

Lyman Continuum Luminosity

- Q or N(H^0) photons/s
- O and B Stars
- AGN
- Central stars of Pne
- Table from Panagia 1973 AJ, 78, 929
- Q = 1.08 x 10^{53} s-1 for SFR = 1 Msun/yr (Kennicutt 1998 ARA&A 36, 189)

	logN_L			
SP	ZAMS	V	III	I
O4	49.93	49.93	49.93	49.93
O5	49.62	49.71	49.71	49.77
O5.5	49.36	49.50	49.53	49.66
O6	49.08	49.24	49.34	49.55
O6.5	48.82	49.02	49.15	49.43
O7	48.62	48.86	49.05	49.37
O7.5	48.51	48.70	49.98	49.34
O8	48.35	48.59	48.90	49.30
O8.5	48.21	48.45	48.83	49.22
O9	48.08	48.32	48.78	49.12
O9.5	47.84	48.08	48.53	48.97
B0	47.36	47.63	47.94	48.53
B0.5	46.23	46.50	46.80	47.60
B1	45.29	45.52	45.87	46.78
B2	44.65	44.89	45.25	46.18
B3	43.69	43.91	44.30	45.57

Pure H Nebula

- Use **Ionization Equilibrium** and Radiative Transfer to describe physical conditions
- What simplications can we make?
- Optically thin
- Optically thick
  - On-the-spot approximation [BB]
  - Ionizations caused by stellar photons are balanced by recombinations to excited levels of H [BB]
  - Stromgren Radius (or Depth) [BB]

Nebulae with H and He

- $T^* < 40,000$ K
- $40,000 \text{ K} < T^* < 100,000$ K
- $T^* > 1e5$ K
  - Central stars of PNe and WR stars

Spectra of Ionized Hydrogen (HII) Regions

Really just these 3 parameters:

- Metallicity
- Spectral Energy Distribution
- Ionization Parameter

Calculate spectrum with radiative transfer codes like CLOUDY or MAPPINGS3

Ionization Parameter

- Let Q = emission rate of Lyman Continuum photons
- $U = Q / (4\pi R_s^2 cn)$, the local ratio of the density of photons to the density of atoms/ions
- Or, $q = Q / (4\pi R_s^2 n) = U * c$
- What is this velocity “q” physically?

Strømgren sphere

O'brock 2.3

· Ionization of a Pure H Nebula

Only radiation with $\nu > \nu_{LL}$ is effective in the photoionization of H from the ground level.

- Write ionization equilibrium equation

$$\int_{\nu_{LL}}^{\infty} \frac{4\pi J_\nu}{h\nu} \sigma\, n(H)\, d\nu = n_{H^+} n_e \alpha_A(H)$$

ionizations / cm^3 / s

Note: $\alpha_A = \sum_{n=1}^{\infty} \alpha_n$

$$\alpha \propto v\sigma \propto v\, v^{-2} \propto v^{-1} \sim T^{-1/2}$$

- Equation of radiative transfer for $\nu > \nu_{LL}$

$$\frac{dI_\nu}{ds} = -\sigma n(H) I_\nu + j_\nu$$

- Convenient to divide ionizing radiation field into two parts

J_ν is per sr, F_ν is not

$$J_\nu = J_{\nu *} + J_{\nu D}$$

$J_{\nu D}$: Emission from Ionized Gas

$J_{\nu *}$: Input Radiation from star

ck ✓ $4\pi J_\nu = \pi B_\nu$ (isotropic / not isotropic)

Stellar Part:

$$4\pi J_{\nu *} = \pi B_{\nu *}(R) = \pi B_{\nu *}(R_*) \left(\frac{R_*}{R}\right)^2 e^{-\tau_\nu}$$

But → $F_\nu = \pi B_\nu$, $4\pi J_\nu = 4\pi \frac{F_\nu}{4} = 4 F_\nu$

$$\tau_\nu(R) = \int_0^R n(H,R)\, \sigma_{ion}(\nu)\, dR$$ optical depth

Diffuse Part – Only recombinations back to n=1 create photons that re-ionize H

$$4\pi \int_{\nu_{LL}}^{\infty} \frac{j_\nu}{h\nu} d\nu = n(H^+)(n_e)\alpha_1$$

$$= 4\pi \int \frac{n_H \sigma J_{\nu D}}{h\nu} d\nu$$

Must Hold Globally

If nebula optically thin → photons escape → $I_{\nu d} = 0$

If nebula optically thick → <u>assume</u> every photon created with $\lambda < \lambda_{ion}$ is immediately absorbed.

$$4\pi \int \frac{j_\nu}{h\nu} dV = 4\pi \int \frac{n_{H^0} \sigma_\nu J_{\nu d}}{h\nu} dV$$

"On The Spot" approximation ⇒ (...same holds locally)

$$J_{\nu d} = \frac{j_\nu}{n_H \sigma_{ion}(\nu)}$$

see O'brock 2.14: b-f Emission coeff.

$$j_\nu(T) = \frac{2h\nu^3}{c^2}\left(\frac{h^2}{2\pi m kT}\right)^{3/2} a_\nu e^{-h(\nu-\nu_0)/kT} n_p n_e$$

why OK?
Because diffuse field photons have $\nu = \nu_0$, so $\sigma(\nu)$ is large + mfp is small.

Eq. Eqn. Becomes

$$\int_{\nu_L}^{\infty} \frac{4\pi J_{\nu *}}{h\nu} \sigma n_H d\nu + \int_{\nu_L} \frac{4\pi J_{\nu D}}{h\nu} \sigma n_H d\nu = n_{H^+} n_e \alpha_A(H)$$

↓ ↓

$$n_H \pi \frac{R_*^2}{R^2} \int \frac{F_\nu(R_*) e^{-\tau_\nu}}{h\nu} \sigma d\nu + 4\pi \int \frac{j_\nu}{h\nu} d\nu = n_{H^+} n_e \alpha_A(H)$$

since $4\pi \int \frac{j_\nu}{h\nu} d\nu = n_{H^+} n_e \alpha_1(H)$

we must have

$$\pi \frac{R_*^2}{R^2} n_H \int \frac{F_{\nu *}(R_*) e^{-\tau_\nu}}{h\nu} \sigma d\nu = n_{H^+} n_e \alpha_B(H)$$

← Note: can integrate this outward to find ionization structure.

where $\alpha_B = \sum_{n=2}^{\infty} \alpha_n$

In optically thick nebulae, the ionizations caused by the stellar radiation-field photons are balanced by recombinations to excited levels of H.

Recombinations to ground level have no net effect on overall ionization balance.

Can integrate outward to find ionization structure.

Integrating out to Stromgren radius, where

$$n_{H^+} \approx n_e \approx n_H \quad \text{for } R < R_S$$

$$n_{H^+} \approx n_e \approx 0 \quad \text{for } R > R_S .$$

$$\int_0^{R_S} \frac{R_*^2}{} \int_{\nu_{ion}}^{\infty} n_H \frac{\sigma}{h\nu} \pi B_{\nu *}(R^*) \frac{}{R^2} e^{-\tau_\nu} d\nu \, 4\pi R^2 \, dR = \int_0^{R_S} n_{H^+} n_e \, \alpha_B(H) \, 4\pi R^2 dR$$

$$4\pi \int_{\nu_{LL}}^{\infty} \frac{\pi B_{\nu *}(R^*) \, R_*^2}{h\nu} \int_0^{R_S} n_H \sigma_{PI} \, e^{-\tau_\nu(R)} \, dR \, d\nu = \int_0^{R_S} 4\pi \, n_{H^+} n_e \, \alpha_B(H) \, R^2 dR$$

$$\tau = \int_0^R n(H) \, \sigma_{ion} \, dR$$

$$\frac{d\tau}{dR} = n(H) \, \sigma_{ion}$$

$$4\pi \int_{\nu_{LL}}^{\infty} \frac{\pi B_*(R_*) R_*^2}{h\nu} \int_0^{R_S} (-1) d(e^{-\tau}) = \frac{4\pi}{3} n_{H^+} n_e \, \alpha_B(H) \, R_S^3$$

$$-e^{-\tau(R_S)} + e^{-0}$$

$$-0 + 1$$

$$4\pi R_*^2 \int_{\nu_{LL}}^{\infty} \frac{\pi B_\nu(R_*)}{h\nu} d\nu = \frac{4\pi}{3} n_{H^+} n_e \, \alpha_B(H) \, R_S^3$$

Lost factor of π here.

$$L_{\nu *} = 4\pi R_*^2 \cdot F_*(R^*)$$

$$= 4\pi R_*^2 \cdot [\pi B_\nu]$$

Size of Stromgren Sphere for Blackbody of Given T_*

$$\frac{4}{3}\pi R_s^3 \alpha_B(H)\, n_{H^+} n_e = Q(H)$$

$$Q = \int_{\nu_{LL}}^{\infty} \frac{L_\nu}{h\nu}\, d\nu$$

$$L_\nu = 4\pi R_*^2 \left[\pi B_\nu\right]$$

$$Q = \int_{\nu_{LL}}^{\infty} 4\pi^2 R_*^2 \frac{2h}{c^2} \frac{\nu^2}{h} \frac{1}{e^{h\nu/kT}-1}\, d\nu$$

$$\boxed{x = \frac{h\nu}{kT}} \qquad dx = \frac{h}{kT}\, d\nu$$

$$= 8\pi^2 \frac{R_*^2}{c^2} \left(\frac{kT}{h}\right)^3 \int \frac{x^2}{e^x-1}\, dx$$

$$R_s^3 = \frac{8\pi^2 R_*^2}{c^2 \frac{4}{3}\pi \alpha_B n_H^2} \left(\frac{kT}{h}\right)^3 \int_{\nu_{LL}}^{\infty} \frac{x^2}{e^x-1}\, dx$$

$$R_s = \left[\frac{8\pi^2 (7\times10^{10}\,\text{cm})^2}{(3\times10^{10}\,\frac{\text{cm}}{\text{s}})^2 \frac{4}{3}\pi (2.6\times10^{-13}\,\text{cm}^3\text{s}^{-1})(1\,\text{cm}^{-3})^2}\right]^{1/3} \frac{kT}{h\nu_{LL}}$$

$$3.289\times10^5\,\text{Hz} \left[\int_{\nu_{LL}}^{\infty} \frac{x^2}{e^x-1}\, dx\right]^{1/3}$$

$$\boxed{R_s = 78.2 \left(\frac{R_*}{R_\odot}\right)^{2/3} n_H^{-2/3} \frac{F_1(x_1)^{1/3}}{x_1}}$$

$$F_1(x_1) = \int_{x_1}^{\infty} \frac{x^2\, dx}{e^x-1}$$

Fig. 2.3

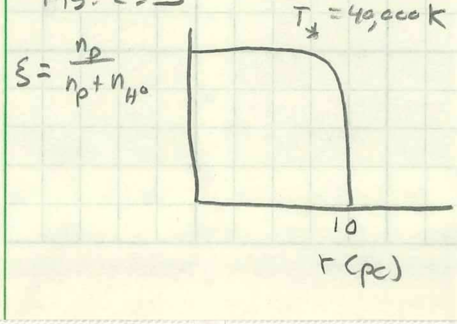

O7.5 V 40,000 K $10^{48}\,\text{s}^{-1}$

Transition Thickness due to absorption = 1 m.f.p of ionizing photon

$$l \sim \frac{1}{n(H^0)\,\sigma_{ion}} \approx 0.1\,\text{pc}$$

$1\,\text{cm}^{-3}$ → $n(H^0)$

THE ASTROPHYSICAL JOURNAL, 525: 321–323, Centennial Issue

STRÖMGREN SPHERES

C. R. O'DELL
Department of Space Physics and Astronomy, MS-108, Rice University, 6100 South Main Street, Houston, TX 77005-1892; cro@rice.edu

1. INTRODUCTION

Bengt Strömgren's 1939 paper marked a watershed in how astronomers view the interstellar medium. The atomic physics employed had essentially all been developed elsewhere, with Strömgren playing a role; but this single publication brought many of the theoretical concepts that had recently been advocated together with new observational results to present a simple and clear picture, i.e., the "Strömgren sphere" nature of the emission-line diffuse Galactic nebulae. Strömgren made many fundamental contributions in other areas, including stellar interiors and spectral-line formation theory, but this work on the eponymous objects is what seems to be mostly remembered today. This simple model of the H II regions dominated our view for nearly four decades, almost to a fault, and the paper that presented it certainly deserves to be ranked as one of the most important in the first century of the American Astronomical Society.

2. ON THE SHOULDERS OF GIANTS

With apologies to Sir Isaac Newton, it is certainly appropriate to use the title to this section to describe the situation in nebular astrophysics at the time of the preparation of Strömgren's 1939 paper. Although this paper is the one that shaped the community's view of the what and why of H II regions, it certainly was not prepared in an intellectual vacuum and drew heavily on the results of others. The supporting work proceeded upon two lines, observational and theoretical.

In this day of splendid color images of the H II regions and photometrically calibrated high-resolution spectra, it is hard to realize how difficult it was to obtain the early spectra and images. The planetary nebulae had become the early targets of spectroscopists (Campbell & Moore 1918), going back to the initial visual observations of William Huggins, because a large number of them had high surface brightnesses, significantly exceeding that of the best known of the H II regions, the Orion Nebula. These observations were coming in on a steady basis, leading to Bowen's (1928) identification of the nebulium lines (they arise from a variety of transitions from ions having the common property of metastable levels lying above ground states within reach of thermal collisional excitation) and motivating theoretical efforts to quantitatively explain the physical conditions and abundances of the planetary nebulae. It was impossible to use the combination of the sensitivity of photographic emulsions with broad bandpass glass filters to isolate individual emission lines, this being long before today's ubiquitous narrowband interference filters. The strongest [O III] lines fell far down on the long-wavelength drop in sensitivity of undyed emulsions, and the Hα emission fell into the low-sensitivity red-dyed spectral region and was contaminated by the straddling [N II] lines. These problems were largely circumvented by the advent of a unique instrument at the site of the McDonald Observatory. This "nebular" spectrograph was actually a "telescopeless" spectrographic system employing one optical elements, it was the perfect device for obtaining well-resolved spectra of low surface brightness large nebulae. Otto Struve & Christian Elvey (1938, 1939) employed this spectrograph to good purpose, demonstrating that extended regions of H II emission were quite common, most of these having well-defined boundaries. At last, one had monochromatic images of the diffuse Galactic nebulae, and they were turning out to have very common properties, i.e., a variety of intrinsic sizes and surface brightnesses, but a common form in having central early-type stars, as well established by Hubble (1922), surrounded by a well-defined outer edge. Although not part of the development of this instrument, Strömgren had spent almost 2 years on the University of Chicago faculty (the latter part in residence at the Yerkes Observatory, where the instrument was built and tested piggyback on the 40 inch refractor) and was fully aware of the incoming results prior to their publication (Osterbrock 1997).

The background theoretical work had developed earlier in the 1930s, and the basic physics was well outlined when Strömgren, together with Gerard Kuiper and Struve (Kuiper, Struve, & Strömgren 1937), considered the ionization state of a low-density gas. The field was advancing rapidly with important papers on the mechanism of production of both permitted and forbidden emission lines at the intellectual hub initiated by Donald Menzel and drawing in the young Lawrence Aller, Leo Goldberg, and James G. Baker. This group's activity continued through the early 1940s and is covered by papers described by Aller (1999) in this special issue (p. 265).

3. THE "STRÖMGREN SPHERE" PAPER

The paper itself is an example of clarity. This must have helped the conclusions reach rapid acceptance, but of course it was the content that led to its long-term significance. There is some difficulty for the modern student of nebular astrophysics in reading it because Strömgren employs the method of formulation of the day, which has subsequently evolved into one where the reader is asked to consider the fate of individual atoms and ions rather than the group properties. Nevertheless, even though armed with the wisdom of hindsight and today's greater knowledge, the reader finds that it is all there.

The primary goal of the paper was to explain the expected variation in the degree of ionization of interstellar hydrogen as a function of distance from a hot star, which is the source of the ionizing photons. Each photoionization is eventually followed by a recombination of the electron and proton to reform neutral hydrogen. The rate at which photoionizations occur depends upon the number of neutral atoms present and the flux of ions capable of lifting the electrons to higher than the ionization potential of 13.6 eV. The rate of recombinations will depend upon the product of the number density of electrons and protons and the electron temperature. The degree of ionization of the hydrogen (x) would be determined by the equality of these two rates, which depend on very different factors. In depth (τ) in the Lyman continuum, a step he had taken earlier (Kuiper et al. 1937). He then develops quantitatively the argument that the degree of ionization will remain almost equal to unity until a critical distance, at which point it drops to almost zero, with the transition distance being small compared with the distance at which the transition occurs. The key factor in this calculation is that τ is proportional to the number of neutral hydrogen atoms between the test point and the ionizing star, this sum being the integral along that line of sight. The results are stated best in Table 2, where one sees how the fraction of hydrogen that remains un-ionized $(1 - x)$ is nearly zero until a critical distance s_0, then rapidly changes to nearly unity. The use of s_0 for designating this distance was consistent with nomenclature of the time that usually called the spatial dimension s, but subsequent investigators quickly began calling this the Strömgren radius. Strömgren then demonstrates how s_0 varies with ionizing star spectral type (Table 5), drawing on the recent bolometric calibration by Kuiper (1938). He clearly states the dependence of s_o on the density (assumed constant).

Except for comparison of the predictions with observed nebulae and estimates of density by other methods, much of the rest of the paper is anticlimactic, being largely a detailed justification of the assumptions made in developing the arguments in § II, establishing their validity in a fashion that remains true today. With today's emphasis on economy of expression, I can imagine the modern referee of the paper commenting that §§ III and IV could be stated in a small fraction of the space! The same comment would probably not have been made about § V, where Strömgren considers how application of this approach to photoionization would lead to a detailed ionization stratification of multielectron atoms, such as oxygen, presaging the detailed calculations now possible through ambitious computer codes such as Gary Ferland's CLOUDY (Ferland et al. 1998). Ferland makes the point often lost by modern consumers of recent computer calculations that the ionization structure of an H II region is determined by the dominant source of opacity, with the ionization structures of the heavy elements being driven by the ionization structure of hydrogen and helium. The labors of creating the modern codes are enormous and their rewards great, but in many ways one can view them as simply cleaning up the details of the Strömgren model. Thank heavens there are those who are doing this valuable work, for the original paper does not suffice to answer today's questions.

Strömgren's paper met with immediate success, in part because of its scientific credibility, but also because he possessed a champion in the influential Otto Struve. This was an important ingredient of its acceptance, since Strömgren had submitted the paper from Copenhagen and remained in isolated Denmark throughout World War II. Struve's Joseph Henry lecture to the Philosophical Society of Washington on "The Constitution of Diffuse Matter in Interstellar Space" (1941) expounds with full credit Strömgren's result within a broader context and in a flowing writing style which can only have helped find acceptance for the young Strömgren's conclusions.

4. HOW THE PARADIGM HAS SHIFTED

That Strömgren's paper has stood the test of time is best measured by the fact that the two most recent texts on the subject of processes in gaseous nebulae (Aller 1984; Osterbrock 1989) both begin their discussions with modern restatements of the Strömgren model. However, those authors and most others today recognize that the inherent simplicity of the Strömgren sphere has led to its application beyond its limits. The common assumption has been that circular symmetry implies spherical symmetry and that in turn is a Strömgren sphere, albeit possibly with a radial density variation. A strong example of the pitfalls of overapplication of an assumption of intrinsic three-dimensional symmetry is the case of modeling the Orion Nebula (M42). Although quite irregular in detail, the object possesses a radial symmetry on the plane of the sky. As densities at various distances became available through observations of the λ3727 doublet ratio of [O II], the results could be compared with the newly derived radio continuum observations. The assumption of spherical symmetry causes one to argue that the object was actually composed of clumps of dense gas, whose volume filling factor varied with radial distance (Osterbrock & Flather 1959). A theoretical dynamical model of the nebula indicated that its sharp density concentration could only be maintained for at most a few tens of thousands of years, inconsistent with the stellar age of the parent cluster (Vandervoort 1964). These spherically symmetric models disappeared in a flash with the blister model of Zuckerman (1973). That model was driven by the fact that the higher ionization potential emission is blueshifted with respect to emission from the ionization front. These motions could not be explained as being due to the symmetric subsonic expansion expected from Strömgren spheres (Lasker 1966); rather, they demanded that the emission came from the flow of gas away from an externally illuminated ionization front located on the surface of a giant molecular cloud (GMC). This model continues to be consistent with most of the other observations of this object (O'Dell 1999) and also must apply to numerous other H II regions (e.g., Mufson et al. 1981), especially the brightest ones.

The existence of these blister-type nebulae is a natural consequence of photoionization that occurs near the surface of a GMC, which would quickly breech the wall of overlying neutral material, and the Strömgren sphere would quickly empty itself (the champagne phase; Tenorio-Tagle 1979) into the lower density surrounds. This would then leave a thin zone of photoionized material through which material would be fed by the host GMC. In retrospect, it is not surprising that most of the optical diffuse Galactic nebulae fit the blister model. If the Strömgren spheres were formed deep inside the GMCs, then there would be so much overlying interstellar extinction that they would appear only in the radio wavelengths. Certainly there is a wealth of such objects (Habing & Israel 1979), and it is mildly ironic that the Strömgren sphere model probably best fits them. The overwhelming selection effect is that we shall see as optical H II regions those photoionization centers formed near the surfaces of the GMC and on the sides facing us.

This evolution of what is considered the best model for the bright optical diffuse Galactic nebulae in no way diminishes the importance of the paper that gave us the Strömgren spheres. The work presented a clear understanding of how photoionized regions operate—one that remains true today, even if the detailed model does not find universal application.

I am grateful to Donald E. Osterbrock for a careful review of this paper and for elaboration of the material included in his history of Yerkes Observatory.

REFERENCES

Aller, L. H. 1984, Physics of Thermal Gaseous Nebulae (Dordrecht: Reidel)

———. 1999, ApJ, 525, 265 (Centennial Issue)

Bowen, I. S. 1928, ApJ, 67, 1

Campbell, W. W., & Moore, J. H. 1918, Pub. Lick Obs., 13, 75

Ferland, G. F., Korista, K. T., Verner, D. A., Ferguson, J. W., Kingdon, J. B., & Verner, E. M. 1998, PASP, 110, 761

Habing, H. J., & Israel, F. P. 1979, ARA&A, 17, 345

Hubble, E. P. 1922, ApJ, 56, 400

Kuiper, G. P. 1938, ApJ, 88, 429

Kuiper, G. P., Struve, O., & Strömgren, B. 1937, ApJ, 86, 570

Lasker, B. M. 1966, ApJ, 143, 700

Mufson, S. L., Fountain, W. F., Gary, G. A., Howard, W. E., III, O'Dell, C. R., & Wolff, M. T. 1981, ApJ, 248, 992

O'Dell, C. R. 1999, in Proc. Ringberg Conf. on Orion, ed. M. J. McCaughrean (San Francisco: ASP), in press

Osterbrock, D. E. 1989, Astrophysics of Gaseous Nebulae and Active Galactic Nuclei (Mill Valley: University Science Books)

———. 1997, Yerkes Observatory, 1892–1950: The Birth, Near Death, and Resurrection of a Scientific Research Institution (Chicago: Univ. Chicago Press)

Osterbrock, D. E., & Flather, E. 1959, ApJ, 129, 26

Strömgren, B. 1939, ApJ, 89, 526

Struve, O. 1941, J. Washington Acad. Sci., 31, 217

Struve, O., & Elvey, C. T. 1938, ApJ, 88, 364

———. 1939, ApJ, 89, 119

Tenorio-Tagle, G. 1979, A&A, 7, 59

Vandervoort, P. O. 1964, ApJ, 139, 869

Zuckerman, B. 1973, ApJ, 183, 163

Dusty HII Regions

Spitzer Fig. 1-1

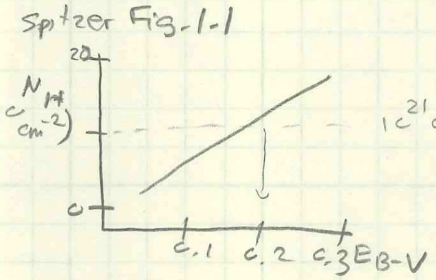

Show History of ISM →

$$\tau_{dust} \approx (2\times10^{-21}\ cm^{-2})\ N_H$$

$$N_H \approx n_H R_S$$

$$\tau_D = 2\times10^{-21}\ n_H R_S \quad , \text{ where } R_S^3 = \frac{Q}{\frac{4}{3}\pi n_H^2 \alpha_B}$$

$$\approx 2\times10^{-21} cm^{-2}\ \frac{n_H\ Q^{1/3} \quad (\sim T/10^4)^{1/3}}{(\frac{4}{3}\pi)^{1/3}\ n_H^{2/3}\ (2.73\times10^{-13}\ cm^3 s^{-1})^{1/3}}$$ where $Q \sim 10^{48} s^{-1}$

See Osterbrock Table 2.3

O star $Q \sim 10^{48} s^{-1}$

$$\approx 0.19 \left(\frac{Q_H}{10^{48} s^{-1}}\right)^{1/3} \left(\frac{n_H}{cm^{-3}}\right)^{1/3} \left(\frac{T}{10^4 K}\right)^{0.23\ 1/6} \qquad \propto Q^{1/3} n^{1/3}$$

⇒ Dust is very important for size of HII regions around O stars ($\gtrsim 10^{48} s^{-1}$) in dense clouds ($n_H \gtrsim 10^3 cm^{-3}$).

Use $\tau = \tau_H + \tau_{Dust}$

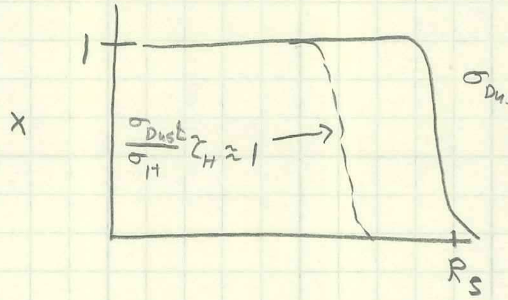

$\sigma_{Dust}/\sigma_H = 0$ ⇒ Decreases size of R_S.

Note: Ionization structure of an HII region is determined by the dominant source of opacity.

See Also ApJ Centennial Issue 525, 321.

Classic Paper: B. Stromgren 1939 ApJ 89, 529.

Brought many theoretical concepts that had been recently advocated together with new observational results to present a clear and simple picture.

See also $T_e(\mathcal{U})$
[D] 15.8

Ionization Parameter

- Consider photoionization eq. of pure H nebula

$$\alpha(T_e)\, n_p n_e = n_{H^0} \int_{\nu_0}^{\infty} \sigma_0 \left(\nu/\nu_0\right)^{-3.5} I_\nu / h\nu \, d\nu$$

$n_e = x\, n$
$n_p = x\, n$
$n_{H^0} = (1-x)\, n$

$$\frac{x^2}{1-x} = \frac{\langle \sigma_{ph} \rangle}{\alpha(T_e)} \frac{S}{n}$$

← photon flux ($\#/cm^2/s$) passing through a unit volume locally

$S = \frac{Q}{4\pi R_s^2}$

$\Rightarrow$ Local ionization state determined by ratio S/n since $\langle \sigma_{ph} \rangle$ and $\alpha(T_e)$ don't vary much among nebulae.

- Physical picture – instead of photoionization eq., consider photon flux S incident on atomic H of density n

photon flux = rate of new ionizations

$$S = \frac{dx}{dt} \cdot n$$

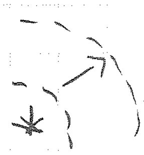

$\Rightarrow$ Ionization parameter $q = S/n$ is the velocity of the ionization front.

- Dimensionless Version

$$\mathcal{U} = \frac{q}{c} = \frac{Q}{4\pi R_s^2 \cdot n c} = \frac{U}{\langle h\nu \rangle \cdot n}$$

- $$\Xi = \frac{P_{rad}}{P_{gas}} = \frac{1}{3} \frac{\langle h\nu \rangle \cdot n\, q}{c} \frac{1}{\frac{3}{2} n k T_e} = \frac{\langle h\nu \rangle \cdot S}{2 c n k T_e}$$

$$= \mathcal{U} \frac{\langle h\nu \rangle}{2 k T_e}$$

DeShave "3" "2" not

↑ energy density, not the total density?

- Stromgren Sphere with H and He

Next most abundant element - He

$$12 + \log \frac{N(He^4)}{N(H)} = 10.99 \quad \text{(Mor tam)}$$

10% by number

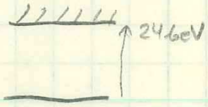

I.P. $He \rightarrow He^+$ 24.6 eV (504 Å)

$He^+ \rightarrow He^{+2}$ 54.4 eV (228 Å) Rare even from O stars WR + PNe

$= 13.6\, Z^2$
$= 13.6\, (2)^2$

* $h\nu > 24.6$ eV can ionize both H and He *

$13.6 \text{ eV} < h\nu < 24.6$ ionize H only

Two types of ionization structure

$f = \frac{H^+}{H}$

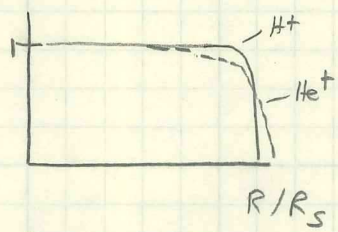

O6 T=40,000

Lots of photons with $h\nu > 24.6$ eV. H^+ and He^+ regions coincide

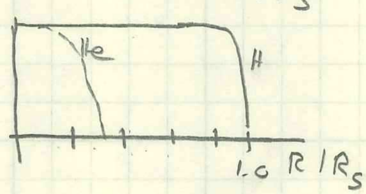

B0 T=30,000

Few photons with $h\nu > 24.6$ eV. Small central He^+ zone compared to H^+ zone.

- Further Iterations on the Ionization Structure

① O.T.S. gives first approximation to ionization distribution.
" " " " " temperature "

② From these, find emission coefficient j_ν throughout the model.

③ From j_ν, find first approximation to $I_{\nu d}$ and J_ν

④ From J_ν, find better approximation to ionization + temperature at each point.

Biggest Shortcoming of OTS: Degree of ionization is so high near the star that ionizing photons emitted there are not really absorbed on the spot. There is a net flow of these photons from the center to the outer regions.

http://thunder.pa.uky.edu/cloudy/

Quantitative Spectroscopy of Ionized Clouds
2003 Ann Rev A & A 41

- Photoionization of He and Heavy Elements

① Direct Ionization

At ionization threshold (504 Å)

$$\sigma_{P.I}(He) = 7.6 \times 10^{-18}\ cm^{-2}$$

$$\sigma_{P.I}(H) = 1.2 \times 10^{-18}\ cm^{-2} = 6.5\times10^{-18}\left(\frac{13.6}{24.6}\right)^3$$

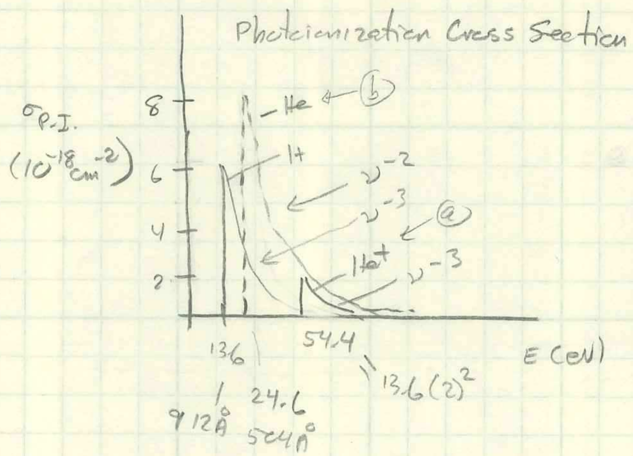

Fig 2.2 Osterbrock
Hummer + Seaton 1963 MNRAS 125, 437

ⓐ See eqn. 2.4 in O'brock from Hummer & Seaton.

For any hydrogenic ion with nuclear charge Z, the P.I. cross section at the threshold is

$$\sigma(\nu_1) = \frac{6.30\times10^{-18}\ cm^{-2}}{Z^2} \quad \text{Roughly } \propto \left(\frac{\nu_1}{\nu}\right)^3$$

$$\sigma(He^+, 54.4 eV) = \frac{6.3\times10^{-18}}{4} = 1.58\times10^{-18}\ cm^{-2}$$

ⓑ @ 24.6 eV (504 Å)

$$\frac{\sigma(He)}{\sigma(H)} = 6.3$$

Why higher cross section? Two (e⁻) targets?
Note: $\sigma(He) \propto \nu^{-2}$ not ν^{-3}

ⓒ Heavier Elements $O\ ^3P\ 1s^2 2s^2 2p^4 \rightarrow O^+\ 1s^2 2s^2 2p^3$
$[^1S, ^1D, ^3P]$ $[^2P, ^2D, ^4S]$

Removal of e⁻ from open shell leads to more than 1 final state. Photoionization cross section increases stepwise w/ energy.

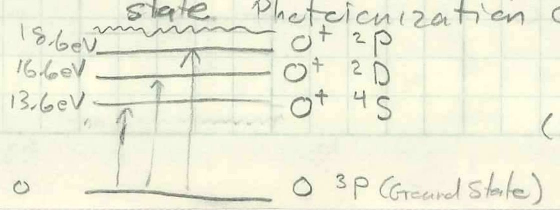

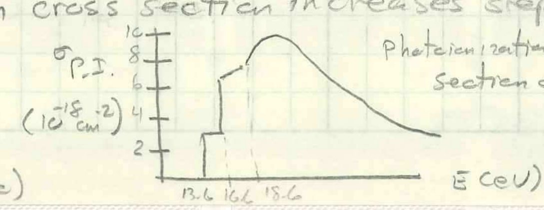

Photoionization cross section of O.

② Autoionization

- Doubly excited states have energy greater than the ionization potential.

Example: He $(1s^2) \rightarrow$ He $(1s2p)$

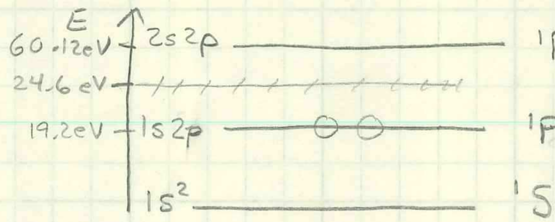

← 19.2eV?

- The doubly excited states can decay non-radiatively into continuum states of $He^+ + e^-$ states.

$He(1s2p) \rightarrow He^+ + e^-$

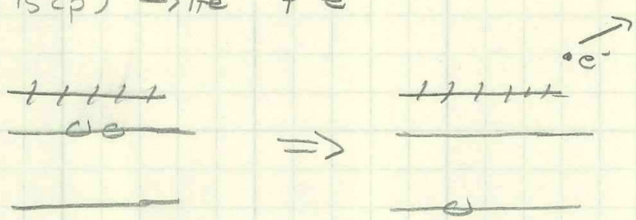

- This is called autoionization and gives rise to resonance spectra.

⊳ see Madden & Codling 1965 ApJ 141, 304.

Fano Profile

60eV is 206 Å

Describe ~20 resonances to excited states

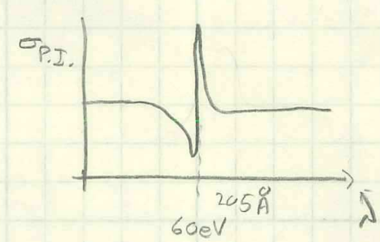

- For He autoionization does not affect cross section much. Can be significant for heavier species; the resonances are smoothed over in diagrams like O'brecht 27.

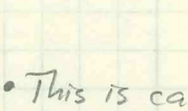

n=1 K shell
n=2 L shell
n=3 M shell

③ Inner Shell Ionizations require x-ray or γ-ray photon. Leaves the other e^-s in excited states

0.599 keV 20.7 Å $\sigma_{P.I.} = 0.44 \times 10^{-18}$ cm^{-2}

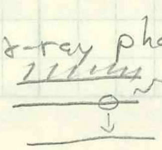

- Helium

Two electrons with spins s_1 and s_2.

Ground State:

Electron Configuration $\underset{\otimes}{1s}$

$$\left.\begin{matrix} m_{\ell_1} = 0 & m_{s_1} = \frac{1}{2} \\ m_{\ell_2} = 0 & m_{s_2} = -\frac{1}{2} \end{matrix}\right\} \quad n=1 \quad L=0 \quad S = 2s+1 = 1$$

$$1\,{}^1S$$

Note $1\,{}^3S$ is not allowed. Requires $m_{n_1} = m_{n_2}$, $m_{\ell_1} = m_{\ell_2}$, $m_{s_1} = m_{s_2}$

why? The two e^-s are called equivalent electrons because they are in the same shell.

Pauli Exclusion Principle – each e^- has a unique set of quantum numbers.

Excited States:

Promote $1e^-$ from 1s orbital to excited ns, np... orbitals
Each configuration gives rise to several <u>spectroscopic terms</u> because there are several possible combinations of m_ℓ, m_s.
Determine LS terms from e^-s in open shells.

e.g. $1s2s \Rightarrow 2\,{}^1S,\ 2\,{}^3S$
$1s2p \Rightarrow 2\,{}^1L \quad 2\,{}^3L$
} non-equivalent e^-s.

Note: $n\,{}^{2S+1}L_J^{\,o}$ ← odd parity

$$\bar{L} = \sum_i \bar{l}_i$$

$$\bar{S} = \sum_i \bar{s}_i$$

$$J = \bar{L} + \bar{S}$$

$$\text{parity} = \sum_i l_i \quad \text{(not a vector sum)}$$

Parity indicates how wave function behaves under reflection of all coordinates through origin

$$\bar{r} \to -\bar{r}$$

Energy Level Diagram:

Singlet He: $S = 0$
Triplet He: $S = 1$

Hund's Rules

1. Terms with larger spin tend to lie lower in energy.
2. Of terms with given configuration and spin, those with largest L tend to lie lower in energy.

He I Energy level Diagram

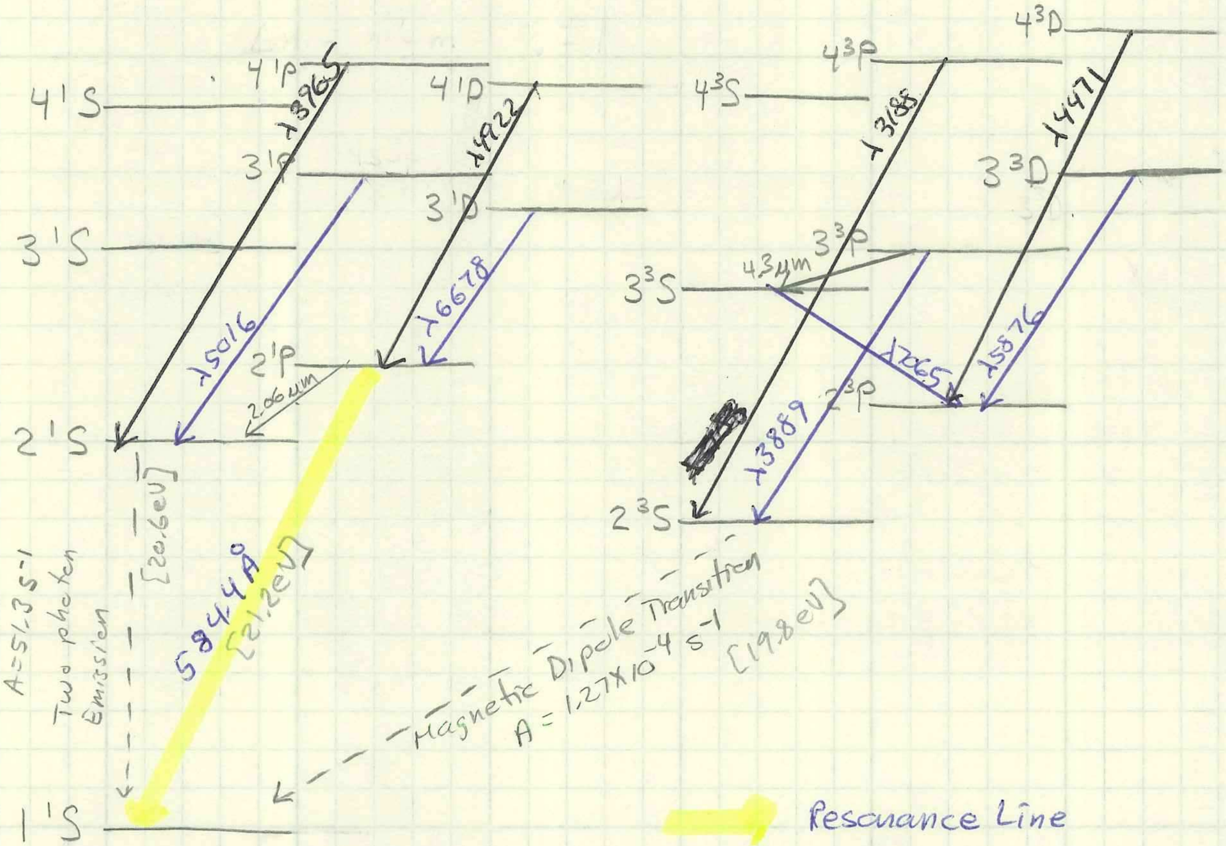

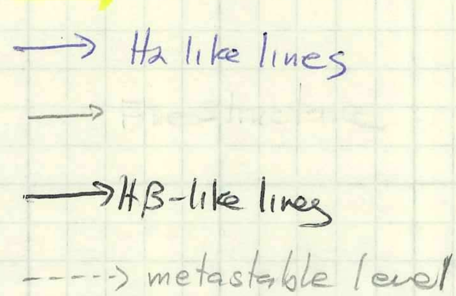

Dipole Selection Rules

$\Delta l = l' - l = \pm 1$
$\Delta m = m' - m = 0, \pm 1$

- Recombination of He and Heavy Elements

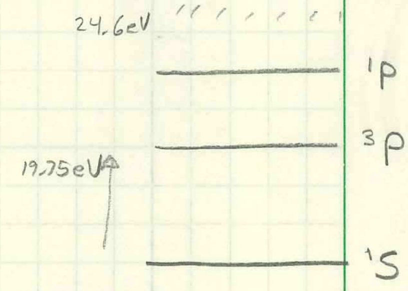

① Radiative Recombination

$He^+ + e^- \rightarrow He^* + h\nu$

ⓐ Rates similar to H:

Recall $\alpha_H(T) \simeq 4 \times 10^{-13} \left(\frac{10^4}{T}\right)^{0.73}$ cm^3 s^{-1}

$\alpha_{He}(T) = 4.3 \times 10^{-13} \left(\frac{10^4}{T}\right)^{0.672}$ cm^3 s^{-1}

$\alpha_{He}(1\,{}^1S, T) = 1.6 \times 10^{-13} \left(\frac{10^4}{T}\right)^{0.48}$ cm^3 s^{-1}

ⓑ Since He is a two-electron system it has separate triplet and singlet states. Recombination rates proportional to statistical weight of each state.

$\alpha_n({}^1L) \approx 1/4\, \alpha_n$

$\alpha_n({}^3L) \approx 3/4\, \alpha_n$

ⓒ Photons emitted during recombination of He^+ can be reabsorbed by H and in most cases ionize H.

ⓓ Same order of magnitude cross-section for heavier elements.

② Dielectronic Recombination –

Inverse of autoionization. Energy released during recombination of 1 e^- excites a ground state e^-: creates

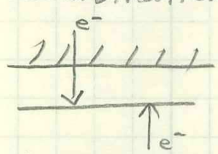

$A^+ + e^- \rightarrow A^{**}$

doubly excited state.

Significantly enhances recombination rate at high T – especially for heavier elements.

• Photoionization of a Nebula with H and He

Photons with $h\nu > 24.6$ eV can ionize either H or He.

1) Recombinations to ground level of He can ionize either H or He. Fraction absorbed by H is

$$y = \frac{N_H\, \sigma(H, \nu_2)}{N_H\, \sigma(H, \nu_2) + N_{He}\, \sigma(He, \nu_2)} \quad \text{where } \nu_2 \gtrsim 24.6\,\text{eV}$$

$1-y$ is the fraction absorbed by He.

2) Recombinations to excited levels of He produce bound-bound transitions. Need to know what fraction can ionize H.

$3/4$ recombine to triplet states $\xrightarrow{\text{radiative}} 2\,^3S \xrightarrow{1\gamma\text{ decay}} 1\,^1S$
metastable; forbidden 19.8 eV, $A = 1.27 \times 10^{-4}\,s^{-1}$

Collisions also are effective in $2\,^3S \rightarrow 2\,^1S$ or $2\,^1P$ transition to further depopulate $2\,^3S$.
Since the collisions leading to the singlet levels involve a spin change, only electrons are effective in causing these excitations.

Note $2^3P \rightarrow 1^1S$ not allowed because $\Delta L = 1$ and $\Delta S = 1$ both, and photon can't carry

$1/4$ recombine to singlet states

of these $2/3$ lead to population of $2\,^1P \rightarrow 1\,^1S$ (most; 21.2 eV resonance line), $\rightarrow 2\,^1S$ (2.06 μm)

$1/3$ lead to population of $2\,^1S \rightarrow 2\gamma \rightarrow 1\,^1S$ emission

$E_{\gamma 1} + E_{\gamma 2} = 20.6$ eV

Per radiative decay from $2\,^1S$ the probability of producing a photon that can ionize H is 0.56 per decay.

$\Rightarrow$ Of the total number of recombinations to excited levels of He per unit volume per unit time is $\alpha_B(He)\, n_{He^+} n_e$, and the fraction p generating (H) ionizing photons is

$$p \approx \frac{3}{4} + \frac{1}{4}\left[\frac{2}{3} + \frac{1}{3}(0.56)\right] = 0.96 \quad \text{In Low Density Limit}$$

$$\approx \left[\frac{3}{4}\underset{\text{to } 2^1S}{(0.78)} + \frac{1}{4}\cdot\frac{1}{3}\right]\underset{2^1S}{(0.56)} + \left[\frac{3}{4}\underset{\text{to } 2^1P}{(0.16)} + \underset{\text{to } 2^1P}{\frac{1}{4}\cdot\frac{2}{3}}\right] = 0.66 \quad \text{HDL}$$

In the O.T.S. approximation, the ionization equations become

① Rate H Ionization From Stellar Photons + Rate H Ionizations from He b-f photons + Rate H Ionizations from He b-b photons = Rate H Recombination to $n \geq 2$

② Rate He Ionization From stellar Photons + Rate of He ionizations from He b-f photons = Rate He recombinations to all levels

Note: Can't assume the $He^+ + e^- \rightarrow He + h\nu$ diffuse field balances He recombinations because some photoionize H.

①
$$n_H \frac{R_*^2}{R^2} \int_{\nu_{LL}}^{\infty} \frac{\pi B_\nu(R_*)}{h\nu} \sigma_\nu(H) e^{-\tau_\nu} d\nu + y\, n_{He^+} n_e \alpha_1(He) + p\, n_{He^+} n_e \alpha_B(He) = n_{H^+} n_e \alpha_B(H)$$

(ν_{LL} = 13.6 eV)

α_1 recombinations Don't produce b-b transition

②
$$n_{He} \frac{R_*^2}{R^2} \int_{\nu_2}^{\infty} \frac{\pi B_\nu(R_*) \sigma_\nu(He) e^{-\tau_\nu} d\nu}{h\nu} + (1-y)\, n_{He^+} n_e \alpha_1(He) = n_{He^+} n_e \alpha_A(He)$$

(ν_2 = 24.6 eV)

$$\frac{d\tau_\nu}{dR} = \begin{cases} n_H \sigma(H), & 13.6 < \nu < 24.6\text{ eV} \\ n_H \sigma(H) + n_{He}\sigma(He), & \nu > 24.6\text{ eV} \end{cases}$$

$$n_e = n_{H^+} + n_{He^+}$$

These equations can be integrated outward step-by-step.

Approximate size found by ignoring the absorption by H in the He^+ zone.
i.e. set $y = 0$ and $n_H = 0$ in $\frac{d\tau}{dR}$ at $\nu > 24.6$ eV.

Then
$$\int_{\nu_2}^{\infty} \frac{L_\nu}{h\nu} d\nu = Q(He) = \frac{4\pi}{3} R_{He}^3 n_{He^+} n_e \alpha_B(He)$$

$\alpha_B(He) = \alpha_A - \alpha_1$

$$Q(H) = \frac{4\pi}{3} R_H^3 \, n_{H^+} n_e \, \alpha_B(H)$$

If He^+ zone much smaller than H^+ zone, then

$n_e \approx n_{He^+} + n_{H^+}$ in He^+ zone

$n_e \approx n_{H^+}$ throughout most of H^+ zone

$$\frac{R_H^3}{R_{He}^3} = \frac{Q(H)}{n_{H^+} n_{H^+}} \frac{\alpha_B(He)}{\alpha_B(H)} \frac{n_{He^+}(n_{He^+} + n_{H^+})}{Q(He)}$$

$$= \frac{Q(H)}{Q(He)} \frac{\alpha_B(He)}{\alpha_B(H)} \frac{n_{He^+}}{n_H} \left(\frac{n_{He} + n_H}{n_H} \right)$$

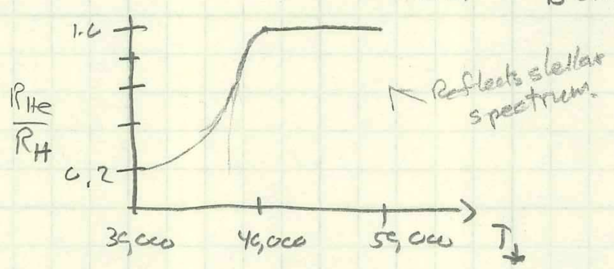

$$\frac{n_{He}}{n_H} \left(\frac{n_{He}}{n_H} + 1 \right)$$